Eur Biophys J (2001) 30: 485–493
DOI 10.1007/s002490100180

ARTICLE

Axel Garbers · Jens Kurreck · Olga Iakovleva
Gernot Renger · Fritz Parak

Mössbauer study of iron centers in D1/D2/Cyt b_{559} complexes isolated from photosystem II of spinach

Received: 19 December 2000 / Revised version: 7 August 2001 / Accepted: 7 August 2001 / Published online: 24 October 2001

Abstract Mössbauer spectroscopy was applied to study the properties of cytochrome b_{559} (Cyt b_{559}) in isolated D1/D2/Cyt b_{559} preparations (from spinach) that are completely deprived of non-heme iron. In these samples, all Cyt b_{559} exists as low-potential form(s) with the iron center attaining the low-spin ferric state in the absence of a strong reductant. The Mössbauer spectra were analyzed using isomer shift and quadrupole splitting parameters below 100 K, gathered from an extrapolation of the temperature dependence of experimental data of photosystem II membrane fragments from spinach. The calculations, based on the Griffith model, lead to the conclusion that the crystal field around the heme iron of Cyt b_{559} is characterized by a strong rhombic distortion. The *g*-values obtained are in agreement with recently published EPR results. The use of an extended theoretical approach permits the description of the relaxation changes of the Mössbauer spectra in the temperature region from 5 K to 60 K. It shows that the environment of the heme iron in D1/D2/Cyt b_{559} is not homogeneous but most likely reflects the existence of two different forms. We assume that factors other than changes of the first coordination sphere are responsible for the drastic negative shift in the redox potential of Cyt b_{559} that takes place during the isolation procedure of D1/D2/Cyt b_{559} complexes. Possible implications of these findings are discussed.

Keywords Cytochrome b_{559} · Mössbauer spectroscopy · Photosystem II · Heme iron

Abbreviations *Chl*: chlorophyll · *Cyt*: cytochrome · *HP*: high potential · *HS*: high spin · *IS*: isomer shift · *LP*: low potential · *LS*: low spin · MC_{TPP}: tetraphenylporphyrinate model complex · *NH*: non-heme · *P680*: photoactive Chl *a* of PS II · *Pheo*: pheophytin · *PS II*: photosystem II · *QS*: quadrupole splitting · *Rps*: *Rhodopseudomonas*

Introduction

The key steps of the photosynthetic cleavage of water into molecular oxygen and metabolically bound hydrogen take place in a membrane-bound multimeric complex referred to as photosystem II (PS II) that acts as a water-plastoquinone oxidoreductase. The overall process of PS II comprises three reaction sequences: (1) light-induced charge separation, leading to the ion radical pair $P680^+Q_A^-$●; (2) sequential two-step formation of PQH_2, with Q_A^-● as reductant, and proton uptake; and (3) sequential four-step oxidation of water to O_2 and four protons, with $P680^+$● as the driving force (for a review see Renger 1999 and references therein). The functional and structural organization of reaction sequences (1) and (2) closely resemble that of anoxygenic purple bacteria while (3) is unique for PS II and takes place at a special manganese-containing catalyst, the water oxidizing complex (WOC). In addition to the WOC, PS II binds another specific component: cytochrome b_{559} (Cyt b_{559}). Rather harsh treatment is required in order to separate this integral constituent from PS II (Garewal and Wasserman 1974; Widger et al. 1984). The tight connection might be indicative of an essential functional and/or structural role of Cyt b_{559}. However, in spite of numerous studies performed during the last three decades (for reviews see Cramer and Whitmarsh 1977; Shuvalov 1994; Whitmarsh and Pakrasi 1996; Stewart and Brudvig 1998), this problem

Dedicated to Prof. E.-G. Jäger (Jena) on the occasion of his 65th birthday

A. Garbers · O. Iakovleva · F. Parak (✉)
Physik Department E17,
Technische Universität München,
85747 Garching, Germany
E-mail: fritz.parak@ph.tum.de
Fax: +49-89-28912548

J. Kurreck · G. Renger
Max-Volmer-Institut für Biophysikalische
Chemie und Biochemie, Technische Universität Berlin,
Strasse des 17. Juni 135, 10623 Berlin, Germany

has not been resolved. Among different possibilities, a protective role against light stress under different conditions is currently discussed to be the most likely function of Cyt b_{559} (Ortega et al. 1988; Thompson and Brudvig 1988; Poulson et al. 1995; Whitmarsh and Pakrasi 1996; Stewart and Brudvig 1998; Gadjieva et al. 1999). This might also include the dissipation of reactive oxygen species like superoxide (Ananyev et al. 1994).

Apart from this important unresolved problem, even the much more simple question about the number of Cyt b_{559} copies bound to PS II is a matter of debate (see Kaminskaya et al. 1999 and references therein). When taking into account the data currently known (Thompson and Brudvig 1988; Poulson et al. 1995; Whitmarsh and Pakrasi 1996; Stewart and Brudvig 1998; Kaminskaya et al. 1999; Sugiura and Inoue 1999 and references therein), it seems likely that there exists a marked difference between cyanobacteria and plants: PS II from the former species contains one Cyt b_{559} and another heme group in the form of Cyt c_{550} (Shen et al. 1995). The recently published structure data on PS II complexes from thermophilic cyanobacteria entirely confirm this conclusion (Zouni et al. 2001). On the other hand, PS II from plants that do not contain Cyt c_{550} can bind two copies of Cyt b_{559} (Garbers et al. 1996). The implications of this difference have to be clarified in future studies.

The most interesting feature of Cyt b_{559} is the remarkable variability of the midpoint potential of the heme group. Cyt b_{559} isolated from plant material exhibits midpoint potentials in the range 115–160 mV (Ortega et al. 1989). In marked contrast, Cyt b_{559} in PS II complexes surrounded by their natural membrane environment exists in different forms with E_m values of about + 400 mV (designated as the HP form), 200 ± 50 mV (IP form) and 60 ± 40 mV (LP form), measured in chloroplasts, thylakoids (Fan and Cramer 1970; Erixon et al. 1972; Horton et al. 1976; Horton and Croze 1977; Rich and Bendall 1980; Ortega et al. 1992; Poulson et al. 1995) and PS II membrane fragments (Ortega et al. 1988; Thompson et al. 1989; Iwasaki et al. 1995; McNamara and Gounaris 1995). A midpoint potential of the order of +400 mV is unique for *b*-type cytochromes. The normalized content of this HP form varies between 50% and 90% and generally decreases under stress conditions such as elevated temperature, detergent and salt treatment, low pH and aging of the sample (Wada and Arnon 1971; Cox and Bendall 1972; Cramer and Whitmarsh 1977; Horton and Croze 1977; Rich and Bendall 1980; Ortega et al. 1990, 1992).

The nature of the structural determinants of the midpoint potential of Cyt b_{559} is not yet clarified. Several factors which affect the redox potential (electric field generated by parallel transmembrane α-helices, dihedral angle between the axial histidine ligands, protonation state of amino acid residues, etc.) have been discussed (Butler 1978; Babcock et al. 1985; Ortega et al. 1988; Krishtalik et al. 1993). These factors considered, the unique coordination of the heme group is most likely responsible for the peculiar redox properties of Cyt b_{559}. The heme iron is usually assumed to attain the low-spin state. This conclusion is based on EPR signals in the range around $g = 3.0$ (Malkin and Vänngard 1980; Nugent and Evans 1980; Bergström and Vänngard 1982; De Paula et al. 1986). However, recently, EPR data were reported that also suggest the existence of high-spin Fe(III) in oxidized Cyt b_{559} (Fiege et al. 1995; Shuvalov et al. 1995; Hulsebosch et al. 1996). This idea is supported by reduced minus oxidized difference absorption spectra monitored in the whole visible region (Kaminskaya et al. 1999).

Mössbauer spectroscopy provides a sensitive tool to analyze the geometry of the ligand field around iron centers (for a review see Schünemann and Winkler 2000). The present study describes an attempt to use this technique in order to investigate the ligand field of the heme iron in Cyt b_{559}. Isolated D1/D2/Cyt b_{559} complexes appear to provide very suitable material because it was shown that these preparations contain only the heme iron of Cyt b_{559} and are lacking the non-heme iron (Kurreck et al. 1997a). The results obtained lead to the conclusion that, in the absence of a strong reductant like $Na_2S_2O_4$, these samples contain two different forms of Cyt b_{559}, with the heme iron in the low-spin ferric state.

Materials and methods

Isolation of PS II preparations

PS II membrane fragments were isolated from spinach grown hydroponically in a ^{57}Fe-enriched medium according to the procedure described in Berthold et al. (1981) with slight modifications as in Völker et al. (1985). D1/D2/Cyt b_{559} complexes were prepared using a modified protocol of Seibert et al. (1988) as outlined in Kurreck et al. (1997a). In order to minimize the Chl content, a washing procedure was carried out until the optical density at 670 nm (OD_{670}) attained values below 0.003. Sensitive silver-stained SDS gels and room temperature absorption spectra exhibited features typical of D1/D2/Cyt b_{559} complexes. The absorption spectrum of the preparations obtained is characterized by a peak maximum in the red at 675 ± 1 nm and a A_{416}/A_{435} ratio of 1.16. This ratio is a characteristic fingerprint for a pure preparation with 6 Chl/2 β-Car/2 Pheo as described in Eickelhoff et al. (1996). All the samples were frozen in small aliquots at liquid nitrogen and stored at temperatures below 200 K.

For Mössbauer measurements the samples have to be concentrated. PS II membrane fragments were centrifuged at 278 K and 165,000×*g*. In the case of ^{57}Fe D1/D2/Cyt b_{559}, the samples were incubated with 25% poly(ethylene glycol) 3350 for 60 min in the dark on ice and subsequently concentrated by ultracentrifugation. The precipitate obtained was transferred into the sample holder of the Mössbauer spectrometer. Complete heme reduction in D1/D2/Cyt b_{559} samples was achieved by dark incubation of the resuspended material with 10 mmol/L $Na_2S_2O_4$ for 20 min.

Mössbauer spectroscopy

The Mössbauer experiments were performed in a weak magnetic field (20 mT) perpendicular to the γ-beam using a ^{57}Co*Rh* source. Details of the equipment and further measuring conditions are described in Parak and Reinisch (1986).

Theory

In a strong octahedral field the five d-electrons of the occupy the t_{2g} manifold, thus representing a state with a single t_{2g} hole with spin $s=1/2$ (Griffith 1957). The pronounced anisotropy of g-values observed in the low-spin (LS) systems, is invoked by a distortion of the crystal field symmetry that is defined by the ligand coordination of the heme iron. Accordingly, measurements of this distortion provide information on the nature and geometry of ligand binding. Our analysis is based on the scheme of the LS ferric state description discussed in detail by Oosterhuis (1971), and on the scheme developed by Afanas'ev et al. (1972) for Mössbauer spectra with a stabilized magnetic hyperfine structure. In contrast to former work, we combined the theory for low-spin Fe^{3+} with a relaxation theory using the Liouville superoperator formalism Afanas'ev and Gorobchenko (1974). We adopt the coordinate system and the equations of Oosterhuis because they allow us the complete and uniform description of all the tensors required within one system.

In the case of rhombic symmetry, the electron system is defined by the spin-orbit coupling constant λ, and by the two crystal field parameters, Δ and V. These parameters account for the axial and rhombic distortions of the cubic symmetry of the crystal field respectively, and are conventionally expressed in units of λ. In other words, Δ characterizes the energy difference between the $|xy\rangle$ orbital and the centre of mass of the $|xz\rangle, |yz\rangle$ orbitals, and V defines the splitting between the $|xz\rangle, |yz\rangle$ orbitals themselves. Spin-orbital coupling mixes the t_{2g} states, and the resulting eigenstates are the three Kramer's doublets (Griffith 1957). Since the magnitude of λ is between 150 and 600 cm^{-1}, only the ground doublet is populated at low temperatures. It is described by Oosterhuis (1971) as:

$$\begin{aligned}\psi_+ &= a|xy\rangle\alpha + b|yz\rangle\beta + ic|xz\rangle\beta \\ \psi_- &= a|xy\rangle\beta - b|yz\rangle\alpha + ic|xz\rangle\alpha\end{aligned} \tag{1}$$

Here α and β are the usual notations for the spin states with spin projections $m_s=1/2$ and $-1/2$ respectively, and a, b and c are the occupation numbers of the hole. The values of a, b and c are unambiguously determined by the parameters Δ and V (Oosterhuis 1971).

It is convenient to substitute the real Hamiltonian operating on the real states (1) with an effective spin Hamiltonian acting on the eigenstates $|\pm 1/2\rangle$ of the effective spin $S=1/2$. Then the spin Hamiltonian of each Kramer's doublet is given in a common way:

$$H = \beta_e B_{ext}\tilde{g}S + I\tilde{A}S + \frac{eQq_{zz}}{4}\left[I_z^2 - \frac{I(I+1)}{3} + \frac{\eta}{3}(I_x^2 - I_y^2)\right] \tag{2}$$

where $\boldsymbol{B}_{ext}$ is the external magnetic field, $\boldsymbol{I}$ the nuclear spin, $\tilde{g}$ the g-tensor, and $\tilde{A}$ the tensor of the hyperfine magnetic interaction. $\tilde{q}$ is the tensor of the electric field gradient with the principal components q_{xx}, q_{yy}, q_{zz}. The quadrupole asymmetry parameter is equal to $\eta = (q_{xx}-q_{yy})/q_{zz}$, and $\Delta E_Q = \frac{1}{2}eQq_{zz}\sqrt{\left(1+\frac{\eta^2}{3}\right)}$ is the quadrupole splitting measured in the absence of the magnetic interaction. We introduce the $\tilde{g}$, $\tilde{A}$ and $\tilde{q}$ tensors rigorously as in appendix A of (Oosterhuis 1971), with the quadrupole asymmetry parameter η included. In order to calculate the magnetic hyperfine interaction, an overall scaling factor P and the Fermi contact factor κ are taken at their typical LS ferric state values of -4.19 mm/s (for the excited state) and 0.35, respectively (Oosterhuis and Lang 1969). With this definition, the paramagnetic hyperfine structure and the quadrupole splitting in a Mössbauer spectrum depend entirely on the values of the crystal field parameters Δ and V.

The application of a weak external magnetic field ($\sim$50 mT) results in the splitting of the Kramers doublet (1), which is much larger than the hyperfine interaction (Afanas'ev et al. 1972). In order to apply the Liouville formalism in the data analysis of the low-spin case, we used the following Hamiltonian of the magnetic hyperfine interaction:

$$H_{hf}^{(\pm)} = \pm^1/_2 G^{-1}(G_x A_x I_x + G_y A_y I_y + G_z A_z I_z) \tag{3}$$

with the parameters A_i ($i=x, y, z$) expressed in units of the hyperfine constant P and with:

$$\begin{aligned}&G_z = g_z\cos\theta,\ G_x = g_x\sin\theta\cos\phi,\ G_y = g_y\sin\theta\sin\phi \\ &G_\pm = G_x \pm iG_y,\ G = \left(G_x^2 + G_y^2 + G_z^2\right)^{1/2}\end{aligned} \tag{4}$$

A similar approach was used by us for the description of the iron-sulfur cluster of HiPIP (Dilg et al. 1999). Furthermore, we take into account the influence of the crystal field fluctuations resulting in the spin relaxation between the sublevels of doublet in Eq. (1). In this case, the effective hyperfine field randomly changes its sign along the z-axis, and the relaxation process is described by a single parameter γ (Van der Woude and Dekker 1965). This influence of relaxation on the Mössbauer spectrum of the LS ferric iron was never treated before and is the subject of the present work. The matrix representation of the Liouville superoperator $\hat{L}$ describing the electron-nuclear system has a block structure in the basis of the electronic functions transformed in the external magnetic field (Afanas'ev et al. 1972; Dilg et al. 1999):

$$\hat{L} = \begin{pmatrix} \hat{L}_{hf} + \hat{L}_Q - \gamma E & \gamma E \\ \gamma E & -\hat{L}_{hf} + \hat{L}_Q - \gamma E \end{pmatrix} \tag{5}$$

where the superoperator $\pm\hat{L}_{hf}$ describes the magnetic hyperfine interaction with the positive or negative projection of the effective hyperfine field, respectively; $\hat{L}_Q$ corresponds to the quadrupole part of the hyperfine interaction, and E is a unit matrix in Liouville space. It is

Eq. (5) that is essential for the interpretation of our Mössbauer experiments.

Results

Figure 1 shows the Mössbauer spectra measured at 155 K of ^{57}Fe-enriched PS II membrane fragments (a) and of isolated D1/D2/Cyt b_{559} complexes either in the absence (b) or in the presence (c) of $Na_2S_2O_4$. These spectra were deconvoluted by a least-squares fit method into quadrupole doublets with Lorentzian lineshape. The results obtained for the values of the isomer shift (IS), quadrupole splitting (QS), linewidth and relative absorption are summarized in Table 1. For comparison, Table 1 also includes the corresponding values obtained for the LS Fe(III) of Cyt *c* in reaction centers from the anoxygenic purple bacterium *Rhodopseudomonas viridis* (Frolov et al. 1991). IS and QS values of other cytochrome *c* types, e.g. of Cyt c_{552} and Cyt c_2 (Moss et al. 1968), are also close to those reported in Table 1. The spectrum of the PS II membrane fragments can be described as a composite of three quadrupole doublets (Petrouleas et al. 1992; Garbers et al. 1996) assigned to three species: two heme irons that differ in their redox state, attaining Fe(II) and oxidized Fe(III) owing to the presence of Cyt b_{559} in the HP and LP forms, respectively, and additionally the non-heme HS Fe(II) iron. The latter is located between Q_A and Q_B on the acceptor side of PS II and coordinated by four histidines (Michel and Deisenhofer 1988) and one bidentate bicarbonate ligand (Hienerwald and Berthomieu 1995). The non-heme iron is accompanied by a minor component with a smaller quadrupole splitting which probably arises from variation in the iron ligation (Petrouleas et al. 1992). The absorption area of this minor component is below 5%, and could not be resolved at 155 K. Figure 1 shows that the Mössbauer spectra of the D1/D2/Cyt b_{559} samples either in the absence or in the presence of $Na_2S_2O_4$ drastically differ from those of the PS II membrane fragments. It has to be mentioned that a minor fraction of about 17% of the Cyt b_{559} cannot be reduced by adding 10 mmol/L $Na_2S_2O_4$ to the resuspended D1/D2/Cyt b_{559} preparation. This indicates the existence of a

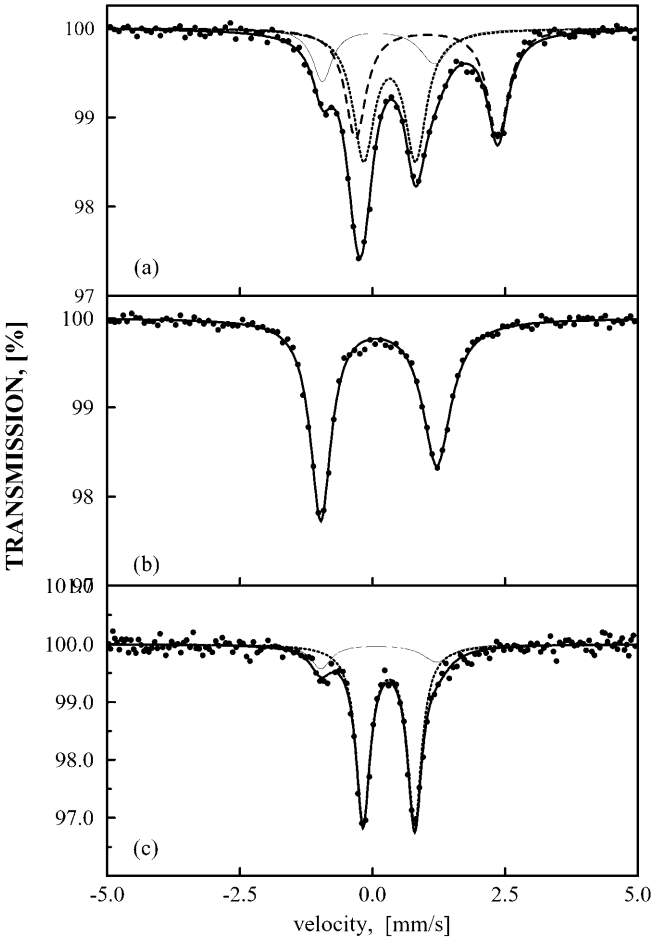

Fig. 1 **a** Mössbauer spectra of ^{57}Fe-enriched PS II membrane fragments; **b** isolated D1/D2/Cyt b_{559} preparations in the absence and **c** in the presence of $Na_2S_2O_4$, measured at $T = 155$ K. The *thin solid line* in **a** and **c** and the *thick solid line* in **b** correspond to the Cyt b_{559} LS Fe(III) species; the *dotted line* corresponds to the Cyt b_{559} LS Fe(II) species and the *dashed line* corresponds to the non-heme Fe(II) HS iron

Table 1 Hyperfine parameters obtained from the Mössbauer spectra of the iron centers in PSII membrane fragments and D1/D2/Cyt b_{559} preparations measured at $T = 155$ K. The fit of the quadrupole doublets is performed on the basis of Lorentzian lineshapes. The bottom line presents the corresponding parameters of the tetraheme Cyt *c* in reaction center crystals from the purple bacterium *Rps. viridis* (Fiege et al. 1995)

Sample	Type of iron center	Isomer shift, IS (mm/s)	Quadrupole splitting, ΔE_Q (mm/s)	Linewidth, $\Gamma/2$ (mm/s)	Absorption area (%)
PS II membrane fragments	Cyt b_{559} Fe(II) LS	0.44 ± 0.01	0.98 ± 0.01	0.49 ± 0.02	45 ± 2
	Cyt b_{559} Fe(III) LS	0.23 ± 0.02	2.12 ± 0.04	0.45 ± 0.04 0.67 ± 0.04	17 ± 2
	Non-heme Fe(II) HS	1.14 ± 0.01	2.68 ± 0.01	0.48 ± 0.02	38 ± 2
D1/D2/Cyt	Cyt b_{559} Fe(III) HS	0.23 ± 0.01	2.17 ± 0.01	0.47 ± 0.01 0.65 ± 0.01	100
	Non-heme Fe	Not detectable			
D1/D2/Cyt	Cyt b_{559} Fe(II) LS	0.43 ± 0.01	0.97 ± 0.01	0.33 ± 0.01	83 ± 2
$+ Na_2S_2O_4$	Cyt b_{559} Fe(III) LS	Fixed values of untreated D1/D2/Cyt b_{559}			17 ± 2
	Non-heme Fe	Not detectable			
Rps. viridis	Cyt *c* Fe(III) LS	0.25	2.12	0.36 0.43	

Cyt b_{559} form with an extra low midpoint potential (XLP form), as outlined by Shuvalov et al. (1994, 1995).

The Mössbauer spectra of the D1/D2/Cyt b_{559} complexes do not show any detectable contribution from a non-heme iron, in agreement with Kurreck et al. (1997a). The measurements also reveal that, in the absence of the exogenous reductant $Na_2S_2O_4$, all iron centers in D1/D2/Cyt b_{559} are present as ferric heme.

Figure 2 shows the temperature dependence of the isomer shift and the quadrupole splitting of the LS ferric center in PS II membrane fragments (Garbers et al. 1998) and in the D1/D2/Cyt b_{559} complex, obtained by a least-squares fit of a sum of Lorentzians. In the case of the PS II membrane fragments, the isomer shift has a very flat and linear temperature dependence. The quadrupole splitting is practically temperature independent up to 250 K. The IS and QS values of the D1/D2/Cyt b_{559} complex are obtained from a fit of the spectra at temperatures $T = 120$ and 155 K. While the IS values are close to those of PS II membrane fragments, the quadrupole splitting is slightly higher than for PS II membrane fragments.

To fit the Mössbauer spectrum of the D1/D2/Cyt b_{559} complex at 5 K, we used supplementary data obtained in measurements at higher temperature and results from EPR spectroscopy reported in the literature. The crystal field parameters Δ and V, which define the magnetic and the quadrupole hyperfine tensors, were chosen so that they correspond to the g-values gathered from EPR spectroscopy for isolated Cyt b_{559} (Babcock et al. 1985; Walker et al. 1986) and D1/D2/Cyt b_{559} complexes (Shuvalov et al. 1995) and from a tetraphenylporphyrinate model complex (MC_{TPP}; Walker et al. 1986). The data are compiled in Table 2. A comparison of the g-values reveals that the EPR measurements monitor two different types of ferric iron centers, both in D1/D2/Cyt b_{559} complexes and in chloroplasts. In the D1/D2/Cyt b_{559} preparations these types are assigned to the LP form with $g_z = 2.93$ and the XLP form with $g_z = 2.91$ (Shuvalov et al. 1995). In chloroplasts, one of the iron centers is again in the LP form with $g_z = 2.94$ while another one is in the HP form with $g_z = 3.08$ (Bergström and Vänngard 1982). For the fit, Eq. (5) was used but without including relaxation. The obtained magnetic

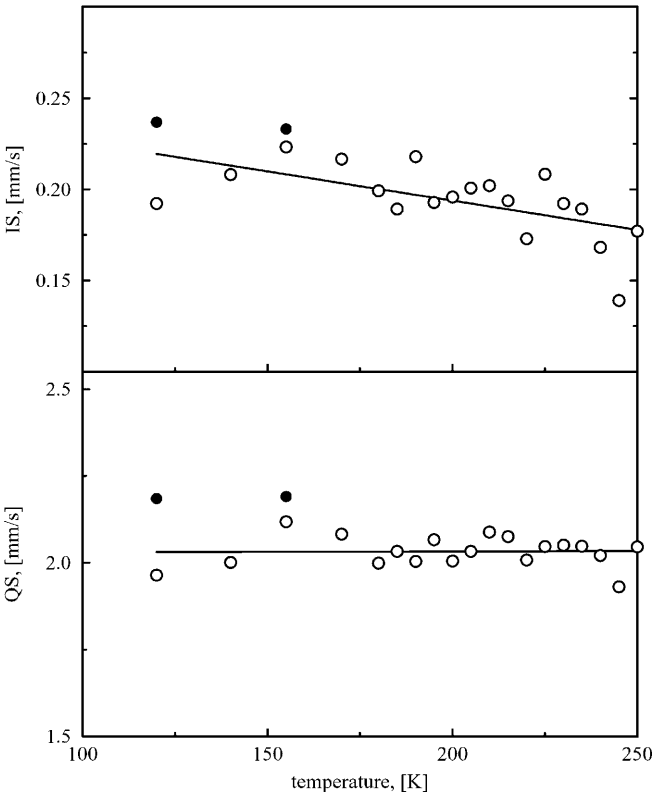

Fig. 2 Temperature dependence of isomer shift and quadrupole splitting for the low-spin Fe(III) heme iron in D1/D2/Cyt b_{559} (*filled circles*) and for PS II membrane fragments (*open circles*)

and quadrupole tensors are summarized in Table 3. In our analysis we assume that the g-tensor and A-tensor share a common principal axis system determined by the geometry around the iron center. The principal axis system of the corresponding q-tensor is rotated around the z-axis of the g-tensor and A-tensor system by the Euler angle $\alpha = 90°$. Figure 3 shows that in this way the Mössbauer spectrum of the D1/D2/Cyt b_{559} sample measured at 5 K in the transverse magnetic field of 20 mT is well described.

In order to describe the temperature dependence of the Mössbauer spectra shown in Fig. 3, it was necessary to use Eq. (5) allowing for relaxation rates. Moreover,

Table 2 Ligand field parameters, g-tensor components and redox properties for Cyt b_{559} in various sample types from higher plants and for MC_{TPP}

Sample/ parameters	D1/D2/Cyt b_{559}[a]	MC_{TPP}[b]	Isolated Cyt b_{559}[c]	D1/D2/Cyt b_{559}[d]		Cyt b_{559} in Chloroplasts[e]	
Δ	3.25	2.88	–	–	–	–	–
V	1.87	0.92	–	–	–	–	–
g_x	1.50	0.85	1.55	1.55	?	?	?
g_y	2.25	1.93	2.26	2.26	2.27	2.26	2.16
g_z	2.93	3.41	2.93	2.93	2.91	2.94	3.08
Redox form	–	–	LP	LP	XLP	LP	HP
E_m (mV)	–	–	230	150	–40	230	370

[a]The values for the D1/D2/Cyt b_{559} sample are the result of the present study
[b]From Babcock et al. (1985)
[c]From Babcock et al. (1985) and Walker et al. (1986)
[d]From Shuvalov et al. (1995)
[e]From Bergström and Vänngard (1982)

two different types of Cyt b_{559} had to be assumed. It has to be emphasized that, in the least-squares fit, all static parameters obtained from the 5 K spectrum were kept constant. Only the relaxation rates were used as variable parameters. This means that the static structure of the Fe(III) irons was assumed to be nearly the same for both Cyt b_{559} molecules. Now, an almost perfect least-squares fit of the theory to the experimental spectra became possible in the whole range of 25 K ≤ T ≤ 60 K (compare Fig. 3). The ratio of the two states with a low-frequency rate, γ_1, and a high-frequency rate, γ_2, respectively, was found to be about 3:2.

Table 3 Hyperfine parameters of the LS Fe(III) iron in D1/D2/Cyt b_{559} calculated from the values of Δ and V in Table 2 (second column). The principal axis system of the quadrupole tensor is rotated by 90° around the z-axis of the molecular axis system

Hyperfine parameters	
q_x, q_y, q_z	–0.50, 0.23, 0.27
A_x, A_y, A_z (in units of P)	–0.65, 0.29, 0.81
Isomer shift (mm/s)	0.23
ΔE_Q (mm/s); η	2.17; –2.68

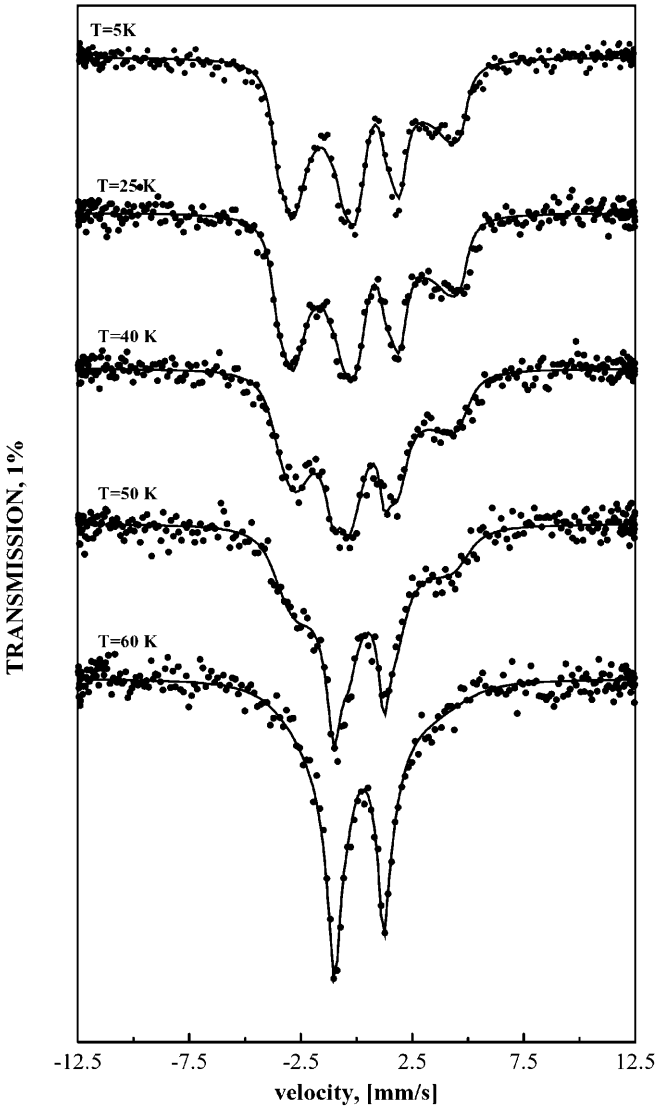

Fig. 3 Experimental and calculated (*solid line*) Mössbauer spectra of D1/D2/Cyt b_{559} at temperatures between 5 K and 60 K. Details of spectral simulation by a model comprising two different spin-lattice relaxation rates are given in the text

The temperature dependence of the relaxation rates γ_1 and γ_2 is shown in Fig. 4. In the available temperature region the data were simulated by:

$$\gamma = C_1 + C_2 \frac{\Delta^3}{e^{\Delta/kT} - 1} + C_3 T^2 \qquad (6)$$

where the first term describes the influence of the spin-spin relaxation, and the second and the third terms account for the spin-lattice relaxation at low and at reasonably high temperatures, respectively. The simulation cannot give unambiguous results because of the small numbers of experiments. Parameters which fit the data are: $C_1 = 1.2\times10^6$ s^{-1}, $C_2 = 2.1\times10^3$ s^{-1} cm^{-3}, $C_3 = 2.7\times10^3$ s^{-1} cm^{-2} for γ_1 and $C_1 = 6.0\times10^6$ s^{-1}, $C_2 = 2.1\times10^3$ s^{-1} cm^{-3}, $C_3 = 33.6\times10^3$ s^{-1} cm^{-2} for γ_2. The energy of the first exited level Δ was taken equal to 380 cm^{-1}, which corresponds to the magnitude of the spin-orbit coupling $\lambda \approx 180$ cm^{-1}.

Discussion

The present study is focused on Mössbauer spectroscopy investigations of the nature and properties of iron centers in the D1/D2/Cyt b_{559} preparation. The results obtained with this sample type and comparative measurements with oxygen evolving PS II membrane frag-

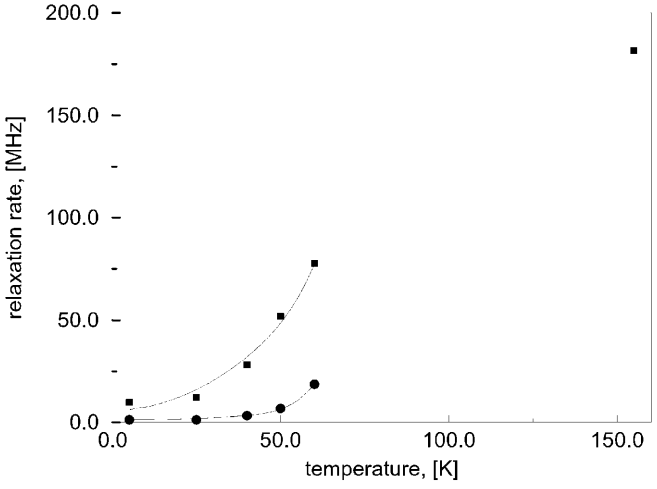

Fig. 4 Temperature dependence of the two spin-lattice relaxation rates obtained from the simulation of the Mössbauer spectra shown in Fig. 3. The low-frequency rate γ_1 and the high-frequency rate γ_2 are shown as *filled circles* and *filled squares*, respectively. The *solid lines* in the low-temperature range reflect the temperature dependence as in Eq. (6)

ments reveal some striking features of the isolated D1/D2/Cyt b_{559} complexes: (1) in terms of the detection limit of Mössbauer spectroscopy, these samples are completely deprived of the non-heme iron, in agreement with Kurreck et al. (1997a); (2) in the absence of strong exogenous reductants (e.g., $Na_2S_2O_4$) all heme irons in the total Cyt b_{559} population of these preparations attain the LS Fe(III) state; and (3) two types of Cyt b_{559} exist that are characterized by a nearly identical environment of the heme group but different dynamic properties of the heme irons.

The loss of the non-heme iron during the preparation procedure severely modifies the geometrical array of the four histidine residues. However, it has to be emphasized that removal of this non-heme iron (NH-Fe) does not necessarily lead to a loss of Q_A, as illustrated for PS II membrane fragments after a thorough extraction of this iron center (MacMillan et al. 1995; Noguchi et al. 1999). On the contrary, a recent FTIR study reveals that the microenvironment of Q_A^-● is only marginally, if at all, disturbed by gentle extraction of the NH-Fe (Noguchi et al. 1999). The loss of the NH-Fe in D1/D2/Cyt b_{559} complexes also excludes the possibility that it might function as internal redox mediator in supporting electron transfer from $Pheo^-$● to exogenous electron acceptors like silicomolybdate.

Reference data for the spectroscopic and redox characteristics of *b*-type heme proteins is provided by the study of well-defined bis-ligated compounds of Fe(III)-porphyrins coordinated to imidazole. The extensive structure analysis of such model complexes has shown that the axial imidazole rings are likely to obtain a coplanar orientation lying parallel or very close to the N_1-N_3 porphyrin vector (Walker et al. 1986). On the contrary, MC_{TPP} favors a perpendicular orientation of the ring planes owing to the steric hindrance of the 2-methyl groups. The distance from the iron ion to the histidine nitrogen is practically unchanged by this hindrance, and is equal to 2.0 Å. The EPR and Mössbauer studies on (imidazole) model complexes have shown that the deviation of the ratio $|V/\Delta|$ from its maximum magnitude of 2/3 is connected with the tilt of the imidazole ring, which destroys the preferred parallel orientation. A parallel orientation of the imidazole ring planes distinguishes energetically the N_1-Fe-N_3 and the N_2-Fe-N_4 axes within the porphyrin ring. The inhomogeneous electrostatic repulsion produced by the axial ligands results in an asymmetrical arrangement of the four heme nitrogens, i.e., in a strong rhombic distortion. A tilt of an imidazole ring lowers the energetic difference and leads to a smaller deviation from a quadratic shape of the heme nitrogen frame. It should be mentioned that in the coordinate system we used, the ratio $\left|\Delta/V\right| \leq 2/3$ is valid (Oosterhuis 1971). The value $|V/\Delta| = 0.58$ of the present study is in agreement with the boundary interval 0.55–0.60 obtained for different *b*-type hems, including isolated Cyt b_{559} (Babcock et al. 1985). In Table 2 the *g*-values calculated from the Hamiltonian parameters Δ and V are compared with the values of different Cyt b_{559} preparations investigated by EPR. It is obvious that the imidazole rings in Cyt b_{559} are aligned parallel to each other. This follows also from a comparison of the *g*-values of D1/D2/Cyt b_{559} and those of the MC_{TPP} model complex and chloroplasts.

From Table 2 one can see that there is no unambiguous correlation between the imidazole rings alignment and the redox properties. On the one hand, two Cyt b_{559} potential forms, LP and XLP, demonstrate a redox shift ~200 mV while the corresponding *g*-values are nearly the same. On the other hand, thermodynamic and crystal field analysis yields a maximal positive shift of ~50 mV (Walker et al. 1986) so far as only the ligand alignment is changed. Although this shift could be essential in the fine tuning of the redox potential of the , it is far too small to describe the observed LP→HP shift.

The Mössbauer spectra of Cyt b_{559} indicate only one type of iron, the low-spin Fe(III) iron with $g_z = 2.93$. This means that the D1/D2/Cyt b_{559} preparation contains the heme group in the LP form (Nanba and Satoh 1987; Garbers et al. 1996; Kurreck et al. 1997b). However, one should keep in mind that the difference between the LP and XLP forms cannot be determined by the Mössbauer technique since the crystal field and hyperfine parameters are indistinguishable. The key to understanding the problem is the presence of two relaxation rates. It proves once more that there are two Cyt b_{559} present where the heme irons have nearly the same chemical environments. However, their dynamic coupling to the thermal bath differs. This indicates distinguishable positions of the two Cyt b_{559} within the complex. It is very probable that the heme with the faster relaxation rate is closer to the hydration shell of the complex. A recent study on Cyt *c* revealed that a variation of the accessibility of the heme group to the aqueous environment gives rise to redox potential changes of more than 200 mV (Tezcan et al. 1998). Accordingly, it is reasonable to assume that a similar effect is also responsible for the existence of the XLP form of Cyt b_{559} in D1/D2/Cyt b_{559} preparations.

Acknowledgements The authors would like to thank L.-E. Andréasson for growing spinach on a ^{57}Fe-enriched medium. The financial support by the Deutsche Forschungsgemeinschaft (Pa 178/14-3 and Re 354/11-3) and the Fonds der Chemie is gratefully acknowledged.

References

Afanas'ev AM, Gorobchenko VD (1974) Shapes of Mössbauer spectra in the rapid-relaxation limit. Soviet Phys JETP 39:690–696

Afanas'ev AM, Gorobchenko VD, Dezi I, Lukashevich I, Filippov NI (1972) Effect of weak magnetic fields on the paramagnetic hyperfine structure of the Mossbauer line in $Fe(ClO_4)_3$. Soviet Phys JETP 35:355–360

Ananyev G, Renger G, Wacker U, Klimov V (1994) The photoproduction of superoxide radicals and the superoxide dismutase activity of photosystem II. The possible involvement of cytochrome *b*559. Photosynth Res 41:327–338

Babcock GT, Widger WR, Cramer WA, Oertling WA, Metz JG (1985) Axial ligands of chloroplast cytochrome *b*-559: identification and requirement for a heme-cross-linked polypeptide structure. Biochemistry 24:3638–3645

Bergström J, Vänngard T (1982) EPR-signals and orientation of cytochromes in the spinach chloroplast thylakoid membrane. Biochim Biophys Acta 682:452–456

Berthold DA, Babcock GT, Yocum CF (1981) A highly resolved oxygen-evolving photosystem II preparation from spinach thylakoid membranes. FEBS Lett 134:231–234

Butler WL (1978) On the role of cytochrome b_{559} in oxygen evolution in photosynthesis. FEBS Lett 95:19–25

Cox RP, Bendall DS (1972) The effects on cytochrome *b*-559HP and P546 of treatments that inhibit oxygen evolution by chloroplasts. Biochim Biophys Acta 283:124–135

Cramer WA, Whitmarsh J (1977) Photosynthetic cytochromes. Annu Rev Plant Physiol 28:133–172

De Paula JC, Li PM, Miller AF, Wu BW, Brudvig GW (1986) Effect of the 17- and 23-kilodalton polypeptides, calcium, and chloride on electron transfer in photosystem II. Biochemistry 25:6487–6494

Dilg AWE, Mincione G, Achterhold K, Iakovleva O, Mentler M, Luchinat C, Bertine I, Parak FG (1999) Simultaneous interpretation of Mössbauer, EPR and ^{57}Fe ENDOR spectra of the [Fe_4S_4] cluster in the high-potential iron protein I from *Ectothiorhodospira halophila*. J Biol Inorg Chem 4:727–741

Eickelhoff C, van Roon H, Groot ML, van Grondelle R, Dekker JP (1996) Purification and spectroscopic characterization of photosystem II reaction center complexes isolated with or without Triton X-100. Biochemistry 35:12864–12872

Erixon K, Lozier R, Butler WL (1972) The redox state of cytochrome *b* 559 in spinach chloroplasts. Biochim Biophys Acta 267:375–382

Fan HN, Cramer WA (1970) The redox potential of cytochromes *b*-559 and *b*-563 in spinach chloroplasts. Biochim Biophys Acta 216:200–207

Fiege R, Schreiber U, Renger G, Lubitz W, Shuvalov VA (1995) Study of heme Fe(III) ligated by OH^- in cytochrome *b*-559 and its low temperature photochemistry in intact chloroplasts. FEBS Lett 377:325–329

Frolov E, Birk A, Fritzsch G, Sinning I, Michel H, Goldanskii VI, Parak F (1991) Mössbauer spectroscopy on the reaction centre of *Rhodopseudomonas viridis*. Hyperfine Interact 68:59–70

Gadjieva R, Mamedov F, Renger G, Styring S (1999) Interconversion of low- and high-potential forms of cytochrome *b*(559) in Tris-washed photosystem II membranes under aerobic and anaerobic conditions. Biochemistry 38:10578–10584

Garbers A, Kurreck J, Reifarth F, Renger G, Parak F (1996) Investigations on the iron of photosystem II membrane fragments. In: Ortalli I (ed) Conference proceedings of ICAME-95, vol 50. Italian Physical Society, Bologna, pp 811–814

Garbers A, Kurreck J, Reifarth F, Renger G, Parak F (1998) Correlation between protein flexibility, electron transfer from $Q_A^{\cdot -}$ to Q_B in PS II membrane fragments from spinach. Biochemistry 37:11399–11404

Garewal HS, Wasserman AR (1974) Triton X-100-4 M urea as an extraction medium for membrane proteins. I. Purification of chloroplast cytochrome b_{559}. Biochemistry 13:4063–4071

Griffith JHE (1957) Binding in hemoglobin azide as determined by electron resonance. Nature 180:30–31

Hienerwald R, Berthomieu C (1995) Bicarbonate binding to the non-heme iron of photosystem II investigated by Fourier transform infrared difference spectroscopy and ^{13}C-labeled bicarbonate. Biochemistry 34:16288–16297

Horton P, Croze E (1977) The relationship between the activity of chloroplast photosystem II and the midpoint oxidation-reduction potential of cytochrome *b*-559. Biochim Biophys Acta 462:86–101

Horton P, Whitmarsh J, Cramer WA (1976) On the specific site of action of 3-(3,4-dichlorophenyl)-1,1-dimethylurea in chloroplasts: inhibition of a dark acid-induced decrease in midpoint potential of cytochrome *b*-559. Arch Biochem Biophys 176:519–524

Hulsebosch RJ, Hoff AJ, Shuvalov VA (1996) Influence of KF, DCMU and removal of Ca^{2+} on the high-spin EPR signal of the cytochrome *b*-559 heme Fe(III) ligated by OH^- in chloroplasts. Biochim Biophys Acta 1277:103–106

Iwasaki I, Tamura N, Okayama S (1995) Effects of light stress on redox potential forms of cyt *b*-559 in photosystem II membranes depleted of water-oxidizing complex. Plant Cell Physiol 36:583–589

Kaminskaya O, Kurreck J, Irrgang KD, Renger G, Shuvalov VA (1999) Redox and spectral properties of cytochrome b_{559} in different preparations of photosystem II. Biochemistry 38:16223–16235

Krishtalik LI, Tae GS, Cherepanov WA, Cramer WA (1993) Redox properties of cytochrome *b*. Biophys J 65:184–195

Kurreck J, Garbers A, Parak F, Renger G (1997a) Highly purified D1/D2/Cyt b_{559} preparations from spinach do not contain the non-heme iron center. FEBS Lett 403:283–286

Kurreck J, Liu B, Napiwotzki A, Sellin S, Eckert H-J, Eichler H-J, Renger G (1997b) Stoichiometry of pigments and radical pair formation under saturating pulse excitation in D1/D2/Cyt b_{559} preparations. Biochim Biophys Acta 1318:307–315

MacMillan F, Lendzian F, Renger G, Lubitz W (1995) EPR and ENDOR investigation of the primary electron acceptor radical anion $Q_A^{\cdot -}$ in iron-depleted photosystem II membrane fragments. Biochemistry 34:8144–8156

Malkin R, Vänngard T (1980) An EPR study of cytochromes from spinach chloroplasts. FEBS Lett 111:228–231

McNamara VP, Gounaris K (1995) Granal photosystem II complexes contain only the high redox potential form of cytochrome *b*-559 which is stabilised by the ligation of calcium. Biochim Biophys Acta 1231:289–296

Michel H, Deisenhofer J (1988) Relevance of the photosynthetic reaction center from purple bacteria to the structure of photosystem II. Biochemistry 27:1–7

Moss TH, Beardon AJ, Bartsch RG, Cusanovich MA (1968) Mössbauer spectroscopy of bacterial cytochromes. Biochemistry 7:1583–1590

Nanba O, Satoh K (1987) Isolation of a photosystem II reaction center consisting of D1 and D2 polypeptides and cytochrome *b*-559. Proc Natl Acad Sci USA 84:109–112

Noguchi T, Kurreck J, Inoue Y, Renger G (1999) Comparative FTIR analysis of the microenvironment in cyanide-treated, high pH-treated and iron-depleted photosystem II membrane fragments. Biochemistry 38:4846–4852

Nugent JHA, Evans MCW (1980) EPR signals of cytochromes in subchloroplast particles. FEBS Lett 112:1–4

Oosterhuis WT (1971) Paramagnetic hyperfine structure: iron complexes with effective spin $S = 1/2$. In: Gruverman IG (ed) Mössbauer methodology, vol 7. Plenum Press, New York, pp 97–121

Oosterhuis WT, Lang G (1969) Mössbauer effect in $K_3Fe(CN)_6$. Phys Rev 178:439–456

Ortega JM, Hervas M, Losada M (1988) Redox and acid-base characterisation of cytochrome *b*-559 in photosystem II particles. Eur J Biochem 171:449–455

Ortega JM, Hervas M, Losada M (1989) Isolation and comparison of molecular properties of cytochrome *b*-559 from both spinach thylakoids and PS II particles. Z Naturforsch C 44:415–422

Ortega JM, Hervas M, Losada M (1990) Distinctive stability of the reduced and oxidised forms of high-potential cytochrome *b*-559 in photosystem II particles. Plant Sci 68:71–75

Ortega JM, Hervas M, Losada M (1992) A possible role for cytochrome *b*-559 in photosynthesis. In: Murata N (ed) Research in photosynthesis, vol 2. Kluwer, Dordrecht, pp 697–700

Parak F, Reinisch L (1986) Mössbauer effect in the study of structure dynamics. Methods Enzymol 131:568–607

Petrouleas V, Sanakis Y, Deligiannakis Y, Diner BA (1992) The non-heme Fe (II) of PSII: (1) binding of new carboxylate anions; (2) study of two Mössbauer components. In Murata N

(ed) Research in photosynthesis, vol 2. Kluwer, Dordrecht, pp 119–122
Poulson M, Samson G, Whitmarsh J (1995) Evidence that cytochrome *b*-559 protects photosystem II against photoinhibition. Biochemistry 34:10932–10938
Renger G (1999) Molecular mechanism of water oxidation. In: Singhal GS, Renger G, Govindjee, Irrgang K-D, Sopory SK (eds) Concepts in Photobiology: photosynthesis and photomorphogenesis. Kluwer, Dordrecht/Narosa, Delhi, pp 292–329
Rich PR, Bendall DS (1980) The redox potentials of the *b*-type cytochromes of higher plant chloroplasts. Biochim Biophys Acta 591:153–161
Schünemann V, Winkler H (2000) Structure and dynamics of biomolecules studied by Mössbauer spectroscopy. Rep Prog Phys 63:263–353
Seibert M, Picorel R, Rubin A, Connolly JS (1988) Spectral photophysical and stability properties of isolated photosystem II reaction center. Plant Physiol 87:303–306
Shen J-R, Vermaas WJF, Inoue Y (1995) The role of cytochrome *c*-550 as studied through reverse genetics and mutant characterisation in *Synechocystis* sp. PCC 6803. J Biol Chem 270:6901–6907
Shuvalov VA (1994) Composition and function of cytochrome *b*559 in reaction centres of photosystem II of green plants. J Bioenerg Biomembr 26:619–626
Shuvalov VA, Schreiber U, Heber U (1994) Spectral and thermodynamic properties of the two hemes of the D1/D2 cytochrome *b*-559 complex of spinach. FEBS Lett 337:226–230
Shuvalov VA, Fiege R, Schreiber U, Lendzian F, Lubitz W (1995) EPR study of cytochrome in the D1/D2 Cyt *b*-559 complex. Biochim Biophys Acta 1228:175–180
Stewart DH, Brudvig GW (1998) Cytochrome *b*559 of photosystem II. Biochim Biophys Acta 1367:63–87
Sugiura M, Inoue Y (1999) Highly purified thermo-stable oxygen-evolving photosystem II core complex from the thermophilic cyanobacterium *Synechococcus elongatus* having His-tagged CP43. Plant Cell Physiol 40:1219–1231
Tezcan FA, Winkler JR, Gray HR (1998) Effects of ligation and folding on reduction potentials of heme proteins. J Am Chem Soc 120:13383–13388
Thompson LK, Brudvig GW (1988) Cytochrome *b*-559 may function to protect photosystem II from photoinhibition. Biochemistry 27:6653–6658
Thompson LK, Miller AF, Buser CA, De Paula JC, Brudvig GW (1989) Characterization of the multiple forms of cytochrome b_{559} in photosystem II. Biochemistry 28:8048–8056
Van der Woude F, Dekker AJ (1965) The relation between magnetic properties and the shape of Mössbauer spectra. Phys Status Solidi 9:775
Völker M, Ono T, Inoue Y, Renger G (1985) Effect of trypsin on PSII particles: correlation between Hill-activity, Mn-abundance and peptide pattern. Biochim Biophys Acta 806:25–34
Wada K, Arnon DI (1971) Three forms of cytochrome *b* 559 and their relation to the photosynthetic activity of chloroplasts. Proc Natl Acad Sci USA 68:3064–3068
Walker FA, Huynh BH, Scheidt WR, Osvath SR (1986) Models of the cytochromes *b*. Effect of axial ligand plane orientation on the EPR and Mössbauer spectra of low-spin ferrihemes. J Am Chem Soc 108:5288–5297
Whitmarsh J, Pakrasi HB (1996) Form and function of cytochrome *b*-559. In: Ort DR, Yocum CF (eds) Oxygenic photosynthesis: the light reactions. Kluwer, Dordrecht, pp 249–264
Widger WR, Cramer WA, Hermodson M, Meyer D, Gullifor M (1984) Purification and partial amino acid sequence of the chloroplast cytochrome *b*-559. J Biol Chem 259:3870–3876
Zouni A, Witt H-T, Kern J, Fromme P, Krauss N, Saenger W, Orth P (2001) Crystal structure of photosystem II from *Synechococcus elongatus* at 3.8 Å resolution. Nature 409: 739–743